TITLE: Electroluminescence and Spectral Shift of CdS Nanoparticles on Si
Wafer

DISTRIBUTION: Approved for public release, distribution unlimited

This paper is part of the following report:

TITLE: Progress in Semiconductor Materials for Optoelectronic
Applications Symposium held in Boston, Massachusetts on November
26-29, 2001.

To order the complete compilation report, use: ADA405047

The component part is provided here to allow users access to individually authored sections
of proceedings, annals, symposia, etc. However, the component should be considered within
the context of the overall compilation report and not as a stand-alone technical report.

The following component part numbers comprise the compilation report:
ADP012585 thru ADP012685

Electroluminescence and Spectral Shift of CdS Nanoparticles on Si Wafer

Eih-Zhe Liang[1], Ching-Fuh Lin[1], Sheng-Ming Shih, and Wei-Fang Su*
Institute of Materials Science and Engineering, National Taiwan University,
Taipei, Taiwan, R.O.C.
[1]Graduate Institute of Electro-Optical Engineering, National Taiwan University,
Taipei, Taiwan, R.O.C.

Abstract

Preparation of CdS nanoparticles, devices fabrication, and electroluminescence properties at room temperature of CdS nanoparticles on silicon substrates are reported. A spectral shift of 86-meV of free exciton transition was observed that was due to the passivation of p-hydroxyl thiophenol molecules around nanoparticles. Controlled process conditions such as heat treatment and/or with oxygen-rich environment are experimented and found to have significant influences on emission spectra. Radiative recombination corresponding to oxygen-impurity level, 273 meV below bandgap energy, presents in samples prepared in oxygen-rich environment. In addition to such mechanism, coalescence of nanoparticles into bulk form also exists and contributes to enhanced luminescence.

Introduction

Low-dimensional structures including nanoparticles or quantum dots (QDs) are supposed to provide significant enhancement in the density of states, so increasing the probability of light emission. Those low-dimensional structures can be epitaxially grown on bulk materials like GaAs wafers or separately formed by chemical methods. The former way is very selective on the grown substrates. Also, QDs are usually formed with only a scarce area density. In contrast, nanoparticles formed by chemical methods have many advantages. First, they can be applied on any substrates. Second, area or volume density of the material can be very high. The process to fabricate monodispersive nanoparticles is inexpensive and facile to industrial application. Stimulated emission and optical gain had been demonstrated in CdS quantum dots by methods of optical pumping[1,2]. This encourages the employment of electrical pumping to realize efficient nanoparticle-based light emitting devices.

In this work, we demonstrate the applications of CdS nanoparticles on silicon substrate. The fabrication of light emitting active layer is simply fabricated by the spin-coating technique. Electroluminescence (EL) can be easily achieved by quantum tunneling of carriers into the nanoparticles. No special care is needed, compared with thermal and chemical budgets of epitaxial technology.

Experimental

Preparation of CdS Nanoparticles

Redissolvable nanoparticles powder of CdS has been synthesized by modifying Pietro's method[3]. Cadmium acetate dihydrate ($Cd(CH_3COO)_2 \cdot 2H_2O$, 0.80 g, 3.0 mmole) was dissolved in a 20 ml mixed solvent of acetonitrile, methanol, and water with a volume ratio of 1:1:2. Another solution containing disodium sulfide nanohydrate ($Na_2S \cdot 9H_2O$, 0.36 g, 1.5 mmole) and p-hydroxyl thiophenol (0.56 g, 4.4 mmole) in the same solvent system was added into vigorously stirred cadmium acetate solution. The whole system was stirred for 18 hours without light illumination. After centrifuging and washing with DI water for several times, we obtained a 0.70g yellow power of CdS nanoparticles encapped by p-hydroxyl thiophenol.

By replacing part of cadmium acetate with manganese acetate (5 %, 10 % and 20 %, in molar ratio), we prepared Mn doped CdS nanoparticles with different concentrations of manganese. All prepared semiconductor nanoparticles can be re-dispersed in ethanol and other polar organic solvents. With ultrasonic vibration and percolation, solutions for spin-coating purpose were produced by dissolving the nanoparicles in ethanol with a concentration of 1% (w/v).

Fabrication of CdS Light-Emitting Diodes on Si

The general fabrication steps of CdS light emitting diodes (LEDs) as follows. First, a low resistivity (doping $\sim 10^{15} cm^3$) silicon wafer was used as the substrate. Acetone, methanol, and DI water were used for subsequently cleaning procedure. The wafer was placed on spinner with several dips of the previously mentioned four CdS and CdS:Mn nanoparticle solutions. A spin speed of 4000 rpm for 60 sec was used. There are three different treatments with the devices. Sample A: The wafer was placed in a chamber, in which 75-mmHg air pressure and room temperature were maintained for 5 minutes to remove ethanol solvents. Sample B: The samples were subsequently treated by rapid thermal annealing (RTA) at 425°C for 5 minutes. The annealing process took place with 75-mmHg air pressure. At this temperature, the organic chemical was decomposed. Sample C: We immersed the CdS nanoparticles into high oxygen concentration environment. The nanoparticle solutions had been separately mixed with SOG (spin-on-glass) 315FX and SiO_2 nanoparticles (average diameter of 12 nm, dissolved in isopropyl alcohol). The cleaned silicon substrate was spin coated with these two kinds of mixture solutions. Both samples were treated by 425°C RTA to sinter the SiO_2 glass.

Subsequently, both top and bottom metal contacts were defined by thermal evaporation. The top semi-transparent contact layer was 10nm gold, and the bottom was 150nm gold. Before the deposition of Au layer, a 3-nm adhesion layer of chromium had been evaporated for both contacts. After voltage bias was applied, EL through top thin layer can be seen by naked eyes. Monochromator(CVI CM110) and photomultiplier were used to record the spectra. In every spectrum measurement, the slit width 0.6 mm was used for maximum detections and correct spectral measurements.

Results and Discussion

The TEM micrograph of CdS nanoparticles is shown in Figure 1(A). The average diameter
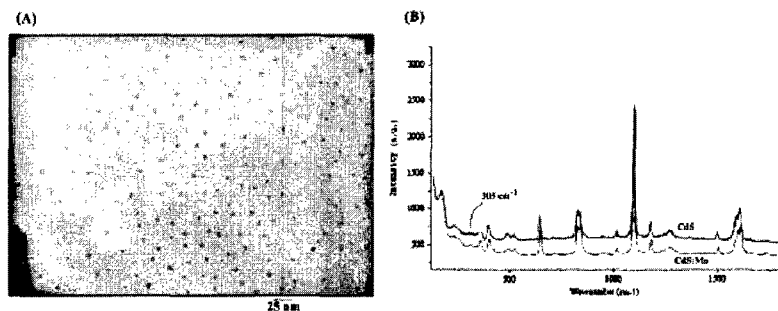

Figure 1. (A) TEM image of p-hydroxyl thiophenol capped CdS nanoparticles and (B) its Raman spectrum as compared with CdS:Mn nanoparticles.

of these spherical CdS nanoparticles is about 5 nm. Compared with the high-temperature synthesizing method by using trioctylphosphine oxygen (TOPO), this room-temperature process is easier but the particle size distribution is wider. In the case of synthesizing manganese doped CdS nanoparticles, we have used large molar percentage of Mn, 5 %, 10 % and 20 % respectively in the reaction. However, only trace doping amounts of Mn, 0.08%, 0.05% and 1.10% were detected respectively by ICP-Mass investigations. When the same approach was used to synthesize MnS nanoparticles, a very low yield was obtained. The results indicate that the reaction rate of MnS synthesis is slower than that of CdS synthesis. Therefore, the position of Cd in the lattice of CdS can not be replaced by Mn. The Mn is trapped by the hydroxyl group of p-hydroxyl thiophenol capping on the surface of CdS nanoparticles. The Raman spectra shown in Figure 1(B) proves this speculation. The Raman shift at 305cm^{-1} corresponds to the longitudinal optical phonons(LO) mode of CdS.[4] No wave number shift is observed for CdS/Mn nanoparticles, thus Mn is not in the CdS lattice. The others Raman shift peaks are from the vibrations of the organic molecules. Consequently, the EL peaks of CdS nanoparticles prepared with or without addition of Mn are the same as shown in Figure 3.

The schematic of CdS-nanoparticle LED is shown in Figure 2(A). The thickness of CdS nanoparticles layer can be as large as 500nm, verified by surface profile scan. Therefore, volume density is very high, but relative high level of resistance also presents. Samples made on n- and p-type Si wafers show different current-voltage (I-V) curves, as shown in Figure 2(B). Both have rectifying I-V curves, but with opposite polarities. This rectifying effect corresponds to metal-insulator-semiconductor tunneling effect. To be specific, the thin potential barrier of organic coating and low substrate doping level result in Schottky-diode-like behavior [5].
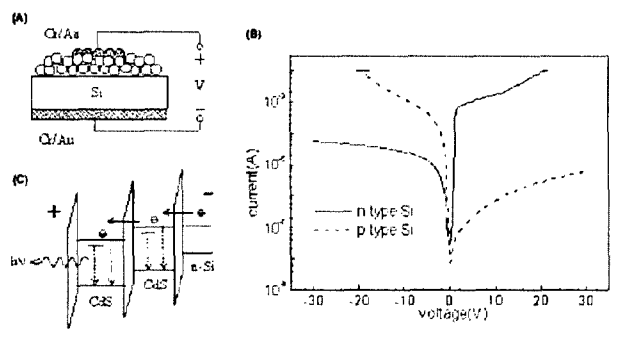
131

Figure 2. (A) Schematic of the CdS nanoparticles EL device on Si wafer. (B) I-V curves of devices on n-type and p-type Si, respectively. (C) Schematic of electron transport and transition in the device.

The EL can be observed only when the devices are forward biased for both types. The carriers injection and current flow for samples on the n-type substrate are illustrated in Figure 2(C). The EL spectra correspond to radiative recombination of carriers confined within CdS nanoparticles. Carriers are supplied by tunneling current. For samples on the n-type substrate, the silicon Fermi level has to be raised so that electrons are able to tunnel through the potential barrier of p-hydroxyl thiophenol group. Within CdS nanoparticles, part of the injected carriers recombine radiatively, part of them get trapped in defect levels, and part of them tunnel into the adjacent nanoparticles.

The turning point around 3V in Figure 2(B) corresponds to the start of carriers recombination process. Only after the applied bias overcoming the potential barrier of p-hydroxyl thiophenol group between the CdS nanoparticle and the metal (or silicon), the radiative recombination process could start.

In the case of sample A, both spectra of CdS and CdS doped with Mn are the same, as illustrated in Figure 3. The anterior observation of Mn in CdS nanoparticle at 585nm(2.119eV) [6] is not clearly observed in our samples. The result is consistent with our ICP-Mass analysis that the Mn atom does not enter into the CdS lattice by our synthesizing method. The emission peak at 526.5nm (2.355eV) is red-shifted from bulk CdS Λ-exciton transition energy, 2.441eV(508nm) at room temperature. [7] The energy with a red-shift of 86 meV does not come from quantum confinement within the nanoparticles, since such effect increases the exciton energy when the particle size decreases [8,9]. It is due to the capping p-hydroxyl thiophenol group that modifies the energy of emission peak. CdS nanoparticles coated with polyvinyl alcohol also show such energy shift in absorption spectrum.[10] Other studies[6,11] have shown different shift level with different coating treatment. The spectrum fits into Lorentzian shape with scattering time of 6 fs.
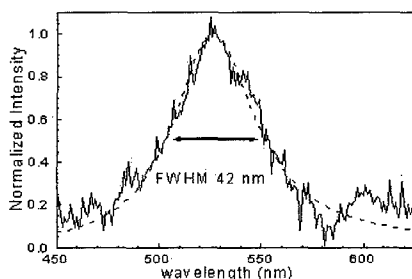
Figure 3. EL Spectrum of CdS with direct vacuum treatment

The FWHM is 42 nm. Such broad spectrum indicates dispersion of particle size. The EL spectrum of sample B depicted in Figure 4(A) shows two peaks. One is at 513.7nm and another at 571.5nm. The former peak stands for bulk CdS signal(A exciton). This spectral lobe can be fitted by Lorentzian shape with scattering time of 8 fs and FWHM 40 nm.

The peak at 571.5nm results from the trapped carriers in oxygen-impurity levels [11]. High temperature environment and the decomposition of p-hydroxyl thiophenol group cause the diffusion process of oxygen into the nanoparticles to occur. This proves p-hydroxyl thiophenol group to be effective overcoat of CdS nanoparticles against oxygen before it decomposes. The oxygen-impurity levels also induce radiative transition.

For investigating the luminescent phenomenon of oxygen impurity level, spectra of the mixture of CdS nanoparticles with SOG and SiO_2 nanoparitcles(sample C) are shown in Figure 4(B). The peak at 513.7nm (2.414eV) is the A exciton signal of bulk CdS at 65°C. The peak at
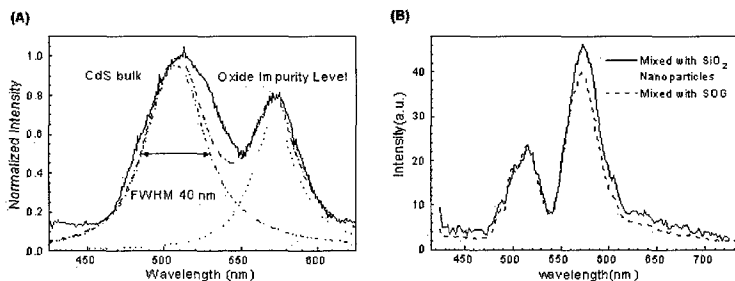

Figure 4. The EL Spectra of (A)CdS particles after heat treatment. (B)CdS nanoparticles mixed with SOG or SiO_2 nanoparticles.

571.5nm (2.414eV) corresponds to radiative transition due to carriers trapped in oxygen-impurity levels, as mentioned previously. The magnitude of light emission in these samples is ten times stronger than that from unheated samples for the same carrier injection condition. The reason for significantly enhanced EL may be twofold. First, the coalescence of CdS nanoparticles into bulk form results in less broadening spectrum around 513.7 nm. Since the potential barrier of p-hydroxyl thiophenol group disappear due to decomposition, carriers in bulk powders stay for enough time (about ns transition lifetime) to recombine radiatively between each tunneling process. Second, relative magnitude of oxygen-impurity-level luminescence is much stronger than that in previous devices. Highly increased concentration of oxygen-impurity levels, which are supplied by SOG or SiO_2 nanoparticles, contributes to the enhancement of internal quantum efficiency. The magnitude difference between mixture with SOG and SiO_2 nanoparticles comes from excess dangling Si-O bond of the latter case. With the same sintering time, the latter mixture makes oxygen diffusing easier.

Conclusions

The CdS nanoparticles prepared by chemical method are ready for spin-coating and EL device fabrication. The observed a spectral shift of free exciton transition of 86 meV is due to the passivation of p-hydroxyl thiophenol group around nanoparticles. Process modifications such as heat treatment and oxygen-rich environment are influential to intrinsic green emission of CdS nanoparticles. The p-hydroxyl thiophenol molecule has shown a protection effect to avoid the diffusion of contaminants into nanoparticels, but it cannot resist temperature deterioration above 400°C. Radiative recombination of carriers trapped in oxygen-impurity levels presents a 273 meV of below bandgap energy of bulk CdS. With the oxygen-impurity levels formed at the surface of CdS nanoparticels, luminescence increases by an order of magnitude.

References

[1] J. Butty, Y.Z. Hu, N. Peyghambarian, Y.H. Kao, and J.D.Mackenzie, Appl. Phys. Lett. **67**, 2672 (1995).
[2] V.I. Klimov, A.A. Milkhailovsky, Su Xu, A. Malko, J.A. Hollingsworth, C.A. Leatherdale, H.-J. Eisler, and M.G. Bawendi, Science **290**, 314 (2000).
[3] J. G. C. Veinot, M. Ginzburg, and W. J. Pietro, *Chem. Mater.* **9**, 2117 (1997)
[4] K.K. Nanda, S.N. Sarangi, S.N. Sahu, S.K. Deb and S.N. Behera, Physica B 262, 31-39(1999).
[5] W.E. Dahlke, and S.M. Sze, Solid-State Electron. 10, 865 (1967)
[6] L. Spanhel, E. Arpac, and H. Schmidt, J. Non. Cryst. Solids **147/148**, 657 (1992).
[7] K.J. Hong, T.S. Jeong, C.J. Yoon, and Y.J. Shin, J. Crystal. Growth. **218**, 19 (2000)
[8] B.G. Potter, Jr. and J.H. Simmons, Phys. Rev. B **37**, 10838 (1988).
[9] M.V Rama Krishna, and R.A. Friesner, J. Chem. Phys. **95**, 8309 (1991)
[10] M. Tanaka, J. Qi, and Y. Masumoto, J. Crystal Growth **214/215**, 410 (2000)
[11] Y. Nosaka, K. Tanaka, and N. Fujii, J. Appl. Polym. Sci. **47**, 1773 (1993)